Microcavity nonlinear optics with an organically functionalized surface

Jin-hui Chen[1] , Xiaoqin Shen[2], Shui-Jing Tang[1,3,4], Qi-Tao Cao[1,3], Qihuang Gong[1,3,4,5], and Yun-Feng Xiao[1,3,4,5,*]

[1] *State Key Laboratory for Artificial Microstructures and Mesoscopic Physics, School of Physics, Peking University, Beijing 100871, China,*

[2] *School of Physical Science and Technology, ShanghaiTech University, Shanghai 201210, China,*

[3] *Frontiers Science Center for Nano-optoelectronics & Collaborative Innovation Center of Quantum Matter, Beijing 100871, China,*

[4] *Collaborative Innovation Center of Extreme Optics, Shanxi University, Taiyuan 030006, China,*

[5] *Beijing Academy of Quantum Information Sciences, Beijing 100193, China.*

This Supplementary Text is organized as follows. In Section I, we introduce the sequential fabrications of the organically functionalized silica microcavity and characterizations. In Section II, the theoretical model is summarized including the dynamic-phase-matching model and discussion of third-harmonic power dependence on the pump power.

I. Sample fabrication and characterizations

The silica microsphere cavity was fabricated from a standard single-mode telecom fiber. The optical fiber was tapered with the pulsed CO_2 laser, and the end of a fiber tip was further melted to form a microsphere with the CO_2 laser illumination. The surface functionalization of a silica microsphere was conducted using modified method [1]. Briefly, a silica microsphere was firstly treated by UV-ozone to generate dense hydroxyl groups on the silica surface. Second, the microsphere was grafted with a coupling layer by using [4-(chloromethyl)phenyl]trichlorosilane by chemical vapor deposition. Third, the as-prepared coupling microsphere was drop-casted with a layer of the 4-[4-diethylamino(styryl)]pyridinium (DSP) molecules, following by thermal treatment at 120°C under vacuum for 20 minutes to accelerate the reaction between DSP and the coupling layer. The microsphere was then cooled to room temperature and rinsed thoroughly with tetrahydrofuran and dried under vacuum at 100°C for 5 minutes, yielding a surface functionalized microsphere. To characterize the thickness of DSP film, the DSP was deposited onto a silicon wafer with the same processes, as aforementioned. The as-fabricated DSP film on a silicon wafer was partly erased by air-laid paper soaked with tetrahydrofuran. The edge profile was measured with KLA-Tencor's P-6 stylus profiler, as shown in Fig. S1.

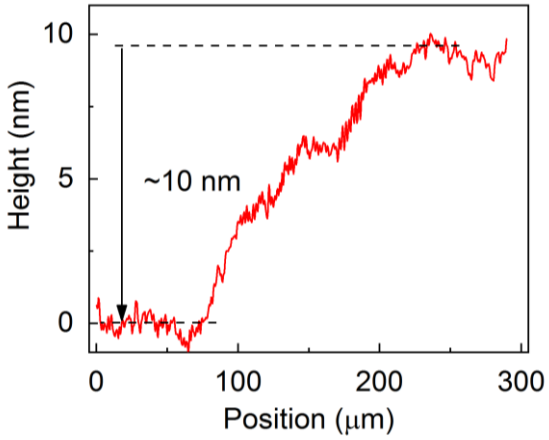

FIG. S1. Edge profile of the DSP film on a silicon wafer.

The photoluminescence spectra of DSP films were measured in a micro-Raman spectrometer in a backscattering configuration. A solid-state 405 nm continuous-wave laser was used as the excitation source with a 405 nm long-pass filter

to block the original laser signal. The backscattered signals were collected through an objective lens and coupled to a spectrometer equipped with a charge-coupled detector working with liquid nitrogen cooling.

Figure S2 shows that the deposition of DSP molecules only slightly degrades the *Q*-factor of microcavities. In terms of the thermal stability, the decomposition temperature for the DSP molecule is about 260 °C [2]. The DSP molecules are stable in dark over one year (in storage) under room temperatures. For the molecule functionalized devices, we did not observe degradation during the storage at room temperatures. When applying high infrared (@1550 nm) pump power ~ 7 mW, corresponding to high intracavity power density ~ 1 GW/cm^2, we did not observe performance degradation. Since the absorption wavelength (~ 470 nm) of the molecules we choose is far shorter than the pump wavelength (1550 nm), it cannot be optically excited at 1550 nm light either under one-photon or two-photon process, which contributes to the high stability of organic molecules under high infrared pump power.

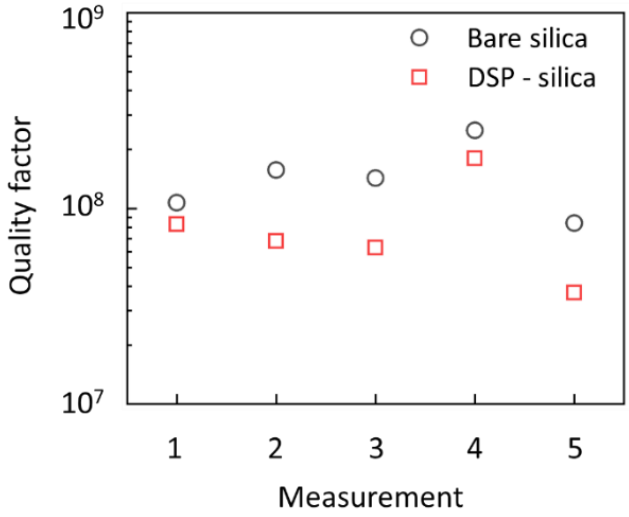

FIG. S2. Measured quality factor distribution of silica microcavities with and without the surface functionalization, showing a slight degradation of *Q*-factor of microcavities after deposition of DSP molecules.

The process of annihilating two pump photons and one Raman Stokes photon to create a visible photon is observed as shown in Fig. S3.

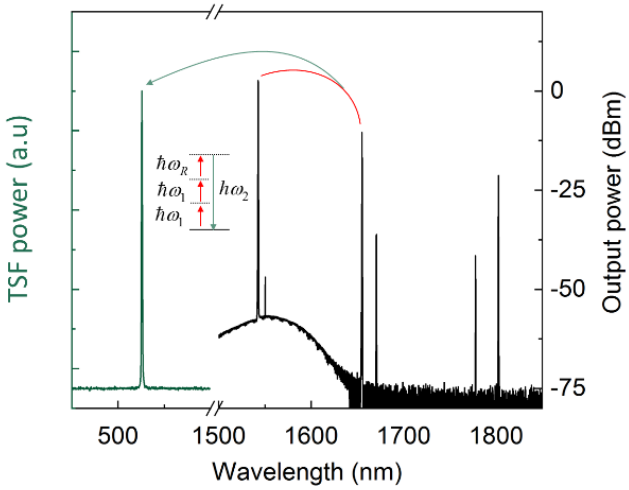

FIG. S3. Measured spectra of Raman-scattering-assisted third-order sum frequency generation. Two pump photons (ω_1, 1542.68 nm) and one Raman Stokes photon (ω_R, 1654.96) are annihilated to create a visible photon (ω_2, 525.79 nm).

II. Theoretical calculations

A. Dynamic phase-matching model

The coupled-mode equation for third harmonic generation (THG) in an optical cavity can be written as

$$\frac{d\tilde{\alpha}_1}{dt} = -i\omega_1\tilde{\alpha}_1 - \frac{\kappa_{10}+\kappa_{1e}}{2}\tilde{\alpha}_1 + \sqrt{\kappa_{1e}}se^{-i\omega_p t} + ig^*\tilde{\alpha}_1^*\tilde{\alpha}_1^*\tilde{\alpha}_2, \quad \text{(S1)}$$

$$\frac{d\tilde{\alpha}_2}{dt} = -i\omega_2\tilde{\alpha}_2 - \frac{\kappa_{20}+\kappa_{2e}}{2}\tilde{\alpha}_2 + ig\tilde{\alpha}_1\tilde{\alpha}_1\tilde{\alpha}_1, \quad \text{(S2)}$$

where the subscripts j=1, 2 indicate the pump and third harmonic (TH) cavity modes with resonance frequencies ω_j respectively; $\tilde{\alpha}_j$ is normalized field amplitude of cavity modes and the $|\tilde{\alpha}_j|^2$ corresponds to the intracavity energy; κ_{j0} and κ_{je} are the intrinsic decay rate and external coupling rate, respectively. $|s|^2$ is the input pump power and g is the third-order nonlinear coupling coefficient between the pump and TH cavity modes, which is defined as

$$g = \frac{9\omega_1^2}{2\omega_2}\frac{\int \boldsymbol{E}_{02}^* \cdot \boldsymbol{P}^{(3)}\, dV}{\int \varepsilon_2 |\boldsymbol{E}_{02}|^2\, dV}, \quad \text{(S3)}$$

where ε_2 is the dielectric constant of TH cavity mode, $\boldsymbol{E}_{02}$ is the normalized electric field distribution of the TH cavity mode, $\boldsymbol{P}^{(3)}$ is the third-order nonlinear polarization, and is defined as $\boldsymbol{P}_i^{(3)} = \Sigma\, \chi_{ijkl}^{(3)} E_{01,j} E_{01,k} E_{01,l}$ where $\chi_{ijkl}^{(3)}$ is the four-order tensor of nonlinear susceptibility, $E_{01,i}$ is the pump mode electric field component. Note that $\boldsymbol{P}^{(3)}$ is composed of the bulk (silica) and surface (DSP) nonlinear response. As a result, the surface effects are routinely modelled by numerically calculating the g factor. In our case, the nonlinearity coefficient is thousands of times larger than that of fused silica [3], the estimated enhancement (Fig. S4) should be two orders of magnitude larger than a bare silica microcavity, which reasonably agrees with the experimental results.

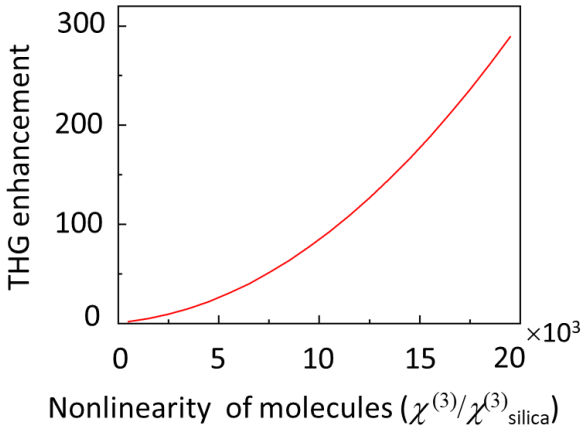

FIG. S4. Theoretical enhancement of THG relating to the organic molecules' third-order nonlinear coefficient $\chi^{(3)}$.

In the rotating frame, $\alpha_1 = \tilde{\alpha}_1 e^{i\omega_p t}$ and $\alpha_2 = \tilde{\alpha}_2 e^{i3\omega_p t}$, thus the coupled-mode equation (S1-S2) can be rewritten as

$$\frac{d\alpha_1}{dt} = [i(\omega_p - \omega_1) - \frac{\kappa_{10}+\kappa_{1e}}{2}]\alpha_1 + \sqrt{\kappa_{1e}}s + ig^*\alpha_1^*\alpha_1^*\alpha_2, \quad \text{(S4)}$$

$$\frac{d\alpha_2}{dt} = [i(3\omega_p - \omega_2) - \frac{\kappa_{20}+\kappa_{2e}}{2}]\alpha_2 + ig\alpha_1\alpha_1\alpha_1. \quad \text{(S5)}$$

Considering the self-phase modulation and cross-phase modulation induced by the thermal and optical Kerr effects [4], we

introduce the parameter B_j to quantitatively characterize the cavity modes shift with the intracavity pump intensity

$$\omega_1=\omega_{10}-B_1|\alpha_1|^2 \tag{S6}$$

$$\omega_2=\omega_{20}-B_2|\alpha_1|^2 \tag{S7}$$

where ω_{j0} is the resonant angular frequency of a cold cavity mode for pump and TH. By substituting equations S6-S7 to S4-S5 and solving the self-consistent equation in the steady state, the dynamic-phase-matching mechanism can be completely revealed. Here we assume that the pump is unperturbed by TH, since the pump light is much stronger than the TH signal. Therefore, the last term in equation S4 can be ignored. The generated TH power (P_2) reads:

$$P_2=\frac{256|g|^2Q_1^6Q_2^2/Q_{1e}^3Q_{2e}}{\omega_1^3\omega_2[4Q_1^2(\frac{\omega_p}{\omega_1}-1)^2+1]^3[4Q_2^2(\frac{3\omega_p}{\omega_2}-1)^2+1]}P_1^3 \tag{S8}$$

where $Q_j=\omega_j/(\kappa_{j0}+\kappa_{je})$ and $Q_{je}=\omega_j/\kappa_{je}$ are the loaded and external quality factor of a cavity mode, respectively; $P_1=|s|^2$ is the pump power.

In Fig. 2 of the main text, the theoretical fitting parameters based on the experimental results are as following: $\omega_{10}/2\pi$=195.4882 THz, $\omega_{20}/2\pi$=586.4438 THz, $Q_1=1.9\times10^7$, $Q_{1e}=3.03\times10^7$, $Q_2=2.5\times10^6$, $Q_{2e}=4.0\times10^6$, $B_1=1.787\times10^{21}$ rad/(J·s), $B_2=4.204\times10^{21}$ rad/(J·s).

B. Third harmonic power dependence on pump power

First, let us consider the case of pump light on resonance ($\omega_p=\omega_1$) which is sufficient for maximized TH output before the reach of critical power (P_c) for the double resonance. By substituting equations S6-S7 into S8, we have

$$P_2=\frac{256|g|^2Q_1^6Q_2^2/Q_{1e}^3Q_{2e}}{\omega_1^3\omega_2[4(\chi_0-\Delta\chi)^2+1]}P_1^3 \tag{S9}$$

where $\chi_0=(3\omega_{10}-\omega_{20})/\gamma_2$ is the initial normalized phase mismatch, γ_2 is the linewidth of TH cavity mode; $\Delta\chi=(3B_1-B_2)|\alpha_1|^2/\gamma_2=4\kappa_{1e}(3B_1-B_2)P_1/[\gamma_2(\kappa_{10}+\kappa_{1e})^2]=\eta P_1$ is the compensation of phase mismatch by the thermal and Kerr effect, $\eta=4\kappa_{1e}(3B_1-B_2)/[\gamma_2(\kappa_{10}+\kappa_{1e})^2]$ is the pump power efficiency for phase mismatch compensation. As a result, we have

$$P_2=\frac{256|g|^2Q_1^6Q_2^2/Q_{1e}^3Q_{2e}}{\omega_1^3\omega_2[4(\chi_0-\eta P_1)^2+1]}P_1^3\ . \tag{S10}$$

From equation S10, it is found that the output TH power (P_2) has an analytical dependence on the pump power (P_1) when $P_1<P_c$ is satisfied. The power dependence of TH on pump is directly decided by χ_0, η and P_1 as discussed in the main text.

As for the case of pump power beyond the critical value ($P_1>P_c$), the power dependence is fundamentally determined by the compromise of phase mismatch of pump light and TH signal. We can have numerical solutions by solving the aforementioned self-consistent equations. By tuning the parameters, the TH curve dependence on the pump could be cubic, nearly-constant and other polynomial as shown in Fig. 5(b) in the main text. For example, when the phase mismatch of TH signal dominates third-harmonic generation process, the P_2 is nearly constant with increase of P_1, which has been explicitly discussed in Fig. 2 of the main text. Interestingly, we find that when $P_1>>P_c$, pump light on resonance ($\omega_p=\omega_1$) is still sufficient for maximized TH output, since the phase mismatch contribution of pump light to the TH signal output is proportional to inverse of third power which is more dominated in THG process. Thus, when $P_1>>P_c$, the equation S10 can be simplified as

$$P_2\sim\frac{64|g|^2Q_1^6Q_2^2/Q_{1e}^3Q_{2e}}{\omega_1^3\omega_2\eta^2}P_1 \tag{S11}$$

The equation S11 shows that the TH power is linear dependence on the pump power when the pump power is far beyond the P_c (Fig. S5).

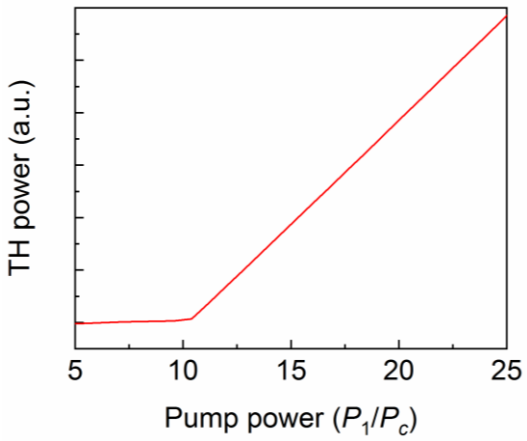

FIG. S5. Theoretical dependence of output TH power on the input pump power.

References

[1] X. Shen, R. C. Beltran, V. M. Diep, S. Soltani, and A. M. Armani, Sci. Adv. **4**, eaao4507 (2018).

[2] F. Pan, M. S. Wong, C. Bosshard, and P. Günter, Adv. Mater. **8**, 592 (1996).

[3] P. Günter, Nonlinear Optical Effects and Materials, (Springer, 2012), Vol. 72, p. 74.

[4] X. Zhang, Q.-T. Cao, Z. Wang, Y.-X. Liu, C.-W. Qiu, L. Yang, Q. Gong, and Y.-F. Xiao, Nat. Photonics **13**, 21 (2019).